CHEMISTRY OF MATERIALS

Communication

pubs.acs.org/cm

High-Yield Alkylation and Arylation of Graphene via Grignard Reaction with Fluorographene

Demetrios D. Chronopoulos, Aristides Bakandritsos, Petr Lazar, Martin Pykal, Klára Čépe, Radek Zbořil, and Michal Otyepka*

Regional Centre of Advanced Technologies and Materials, Department of Physical Chemistry, Faculty of Science, Palacký University Olomouc, tř. 17. listopadu 12, 771 46 Olomouc, Czech Republic

Supporting Information

Covalent functionalization of graphene significantly broadens its application potential via tuning its electronic and surface properties.[1,2] Therefore, a wide range of dry and wet chemistry approaches have been developed for graphene functionalization.[3−7] Despite recent progress in this field, covalent modification of graphene is still hampered by its low reactivity. Moreover, the reactivity depends on the type of graphene support[8,9] and number of graphene layers.[10−12] Consequently, there is a need for new strategies that permit high yielding graphene functionalization under more controlled conditions.

Very recently, fluorographene (FG), a stoichiometric (C_1F_1) and well-established graphene derivative,[13−18] has been shown to be susceptible to reductive defluorination[14] and nucleophilic attack.[19] These findings suggest that FG may be a useful alternative material to graphene for the preparation of graphene derivatives. This idea is supported by recent achievements in the field employing nucleophilic substitution of fluorine atoms by other groups, such as sulfhydryl,[20] amino,[21−24] alkoxy,[22] dichlorocarbene[25] and urea.[26] However, efficient reaction of FG with Grignard reagents to allow high yield alkylation and arylation of graphene has not yet been reported.

The Grignard reaction is one of the most well-established methodologies for the formation of C−C bonds in organic chemistry. Grignard reagents bear a nucleophilic carbon atom owing to its bonding to magnesium, and the in situ formed hydrocarbon anion can attack electrophilic carbons, such as the carbons of FG.[19,22] The Grignard reaction has been successfully applied to fluorinated carbon nanotubes,[27] but to date, there is only one report regarding the covalent modification of chlorinated graphene with Grignard reagents.[28] Very recently, the same group reported that Grignard reaction on fluorinated epitaxial graphene was not feasible.[29]

In the present work, we report the first successful covalent modification of FG based on the Grignard reaction, which yielded homogeneous and high-density (5.5−11.2%) functionalization of the graphene surface. Three different types of organometallic reagents, containing alkane (pentyl), alkene (allyl), and aryl (anisolyl or *p*-methoxyphenyl) moieties, reacted successfully, unlike the reaction with the ethynyl reagent. This behavior was rationalized in terms of the nucleophilicities of the reactive centers, assessed by computational chemistry (Figure 1). The new covalently functionalized graphene derivatives were characterized by complementary techniques: spectroscopic, thermogravimetric and microscopic. In addition, we used density functional theory (DFT) calculations to evaluate

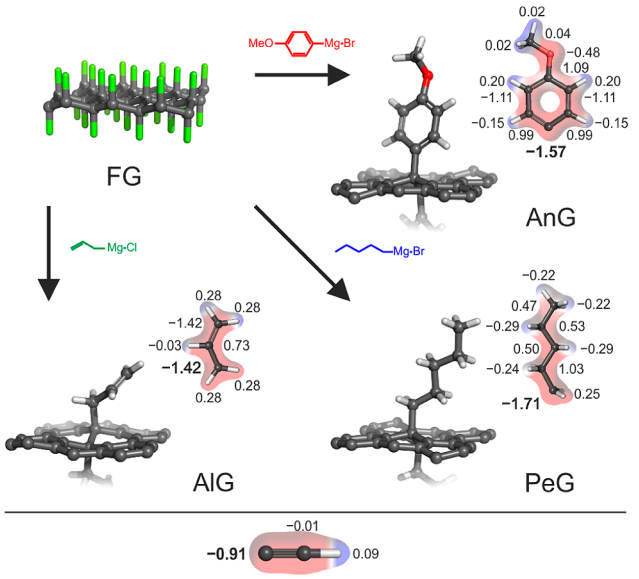

Figure 1. Overview of the reaction of fluorographene with Grignard reagents, yielding covalently functionalized graphenes. The partial charges on the nucleophilic carbons in the hydrocarbon anions are shown in bold.

the thermodynamic stabilities of the chemically modified graphenes, and delineate the influence of the different covalently attached groups on the electronic properties of graphene.

Initially, a FG suspension was prepared by sonication of graphite fluoride (GF) in dry tetrahydrofuran. Next, the Grignard reagent (Figure 1) was added dropwise to the suspension and the mixture was stirred under nitrogen for 5 h. Afterward, excess Grignard reagent was quenched with a saturated aqueous solution of ammonium chloride and the material was washed with a copious amount of water. To remove any residues of magnesium salts, the product was resuspended in aqueous 5% HCl solution and washed with water, ethanol and dichloromethane, consecutively.

When ethynylmagnesium bromide was used as a precursor compound for the generation of the nucleophile (ethynyl group), the reaction with FG was unsuccessful, even after

Received: November 27, 2016
Revised: January 6, 2017
Published: January 29, 2017

DOI: 10.1021/acs.chemmater.6b05040
Chem. Mater. 2017, 29, 926−930

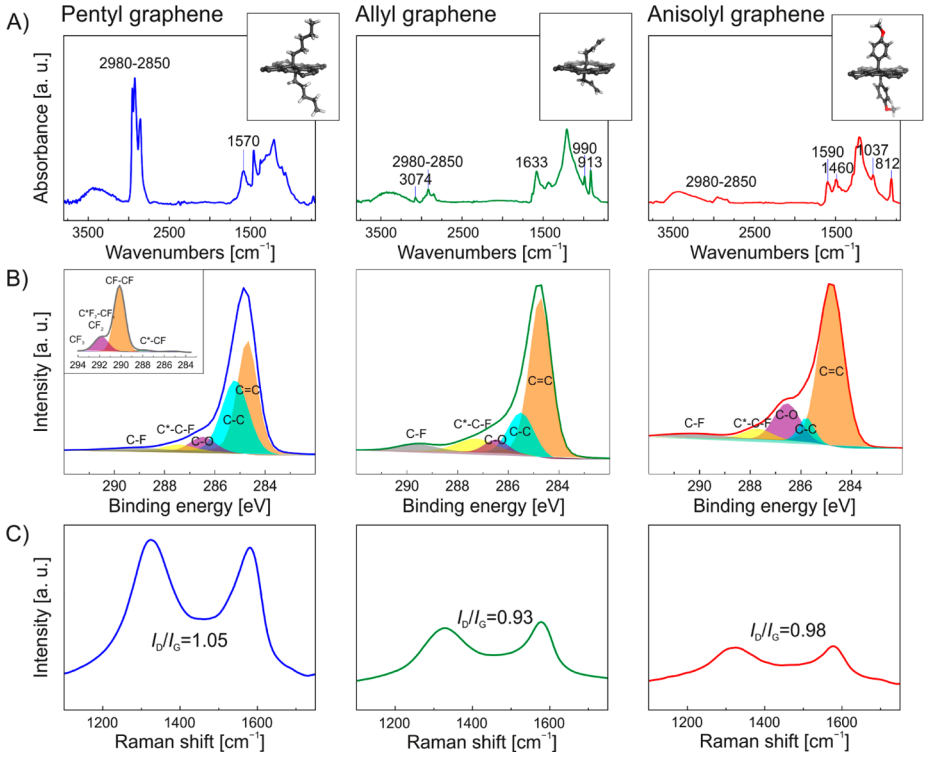

Figure 2. FT-IR (A), C 1s XPS (B) and Raman (C) spectra of graphene derivatives. The inset (left panel B) shows the XPS spectrum of pristine GF.

heating at 60 °C. To decipher this result, DFT calculations were carried out to assess the nucleophilicity of the reacting hydrocarbon anions in terms of the electrostatic potential-derived partial charges. The calculations indicated that the electrostatic potential over the nucleophilic ethynyl carbon was the lowest among the considered nucleophiles (Figure 1). It should be noted that our DFT calculations indicated that ethynyl was thermodynamically stable on graphene owing to the formation of a strong covalent bond to graphene with high binding energy of −2.40 eV. This implies that the unsuccessful outcome of the reaction was due to kinetic reasons.

Successful covalent functionalization of FG by Grignard reagents was confirmed by Fourier transform infrared (FT-IR) spectroscopy, owing to the appearance of new bands, not present in pristine GF (Supporting Information, Figure S1A). Aliphatic C—H stretching vibrations were found at 2980−2850 cm^{-1} for the alkyl-, alkenyl- and aryl-functionalized graphenes (Figure 2A). In particular, the spectrum of allyl graphene (AlG) displayed four unique bands at 3074, 1633, 990 and 913 cm^{-1}, which were ascribed to the monosubstituted alkene group. Concerning the anisolyl graphene (AnG), bands due to the C—O bond and *para* disubstitution of the benzene ring were observed at 1037 and 812 cm^{-1}, respectively. Moreover, the FT-IR spectra showed the presence of aromatic rings due to the occurrence of two characteristic bands at around 1590 and 1460 cm^{-1}. The band at 1570 cm^{-1} was particularly evident for the pentyl graphene (PeG), and corresponded to conjugated C═C double bonds, which were formed owing to the reductive defluorination[14,30] of FG occurring simultaneously with the substitution.

All graphene derivatives showed almost quantitative elimination of fluorine atoms according to atomic content analyses obtained from X-ray photoelectron spectroscopy (XPS) survey spectra (Supporting Information Figure S1B, and Table S1). High-resolution C 1s XPS spectra of the covalently functionalized graphene derivatives (Figure 2B) showed that the intensities of the C−F_x components at binding energies of 288−293 eV were significantly reduced with respect to FG (Figure 2B inset, and Table S2). Moreover, the appearance of a band at 284.7 eV for all materials, which was absent in the starting GF material, confirmed the presence of sp^2 carbons formed as a result of defluorination. Regarding AnG, the oxygen content was found to be 8.3% (Supporting Information, Table S2) owing to the presence of oxygen atoms in the anisolyl (*p*-methoxyphenyl) functionality, verifying successful attachment of this group to the carbon lattice.

Formation of conjugated double bonds in all three graphene derivatives was also confirmed by Raman spectra. Whereas the starting material was Raman silent,[25] the Raman spectra of the graphene derivatives exhibited characteristic D and G bands at around 1330 and 1580 cm^{-1}, respectively (Figure 2C). The ratio of I_D and I_G band intensities (I_D/I_G, which reflects the degree of functionalization) for pentyl, allyl and anisolyl graphene was 1.05, 0.93 and 0.98, respectively. These values, along with considerable broadening of the bands, indicate a high degree of graphene functionalization.[31,32] Similar broadening occurred for the 2D band (Figure S2), restricting the evaluation of the number of the layers in the derivatives. All these observations suggest that the treatment of FG with Grignard reagents generated covalently and high-density functionalized graphenes, formed via nucleophilic substitution and accompanied by reductive defluorination. The concurrent substitution and defluorination resulted in materials with negligible fluorine content which could be considered as graphene alkanes and alkenes, or aryl graphenes. Therefore, the reported strategy, i.e., functionalization of FG by nucleophiles, represents an efficient and robust alternative approach for the direct functionalization of graphene.

To estimate the thermal stability and functionalization degree of the graphene derivatives, thermogravimetric analysis (TGA)

DOI: 10.1021/acs.chemmater.6b05040
Chem. Mater. 2017, 29, 926−930

was employed under nitrogen. The starting material is known to be stable below 400 °C and exhibits weight loss of 75% in the temperature range 450−650 °C,[13] as also shown in Figure S3. The TGA profiles indicated that decomposition of PeG started at 180 °C, whereas AlG and AnG derivatives started to decompose at higher temperatures (220 °C). These observations suggest that the alkyl-graphene derivative was less stable than the alkenyl and aryl derivatives. DFT calculations corroborated the TGA results because they revealed that the binding energy of pentyl on graphene was 0.54 eV per molecule, whereas the binding energies of allyl and anisolyl were higher, i.e., 0.81 and 0.91 eV.

According to the theoretical calculations, the grafting of functional groups onto FG reduced its band gap (BG) from ∼8 eV[33,34] to ∼0.15 eV (Figures 3A, and S4), suggesting them as small-BG semiconductors. The BG was direct and narrowed with decreasing coverage (Figure S4). The BG occurred due to

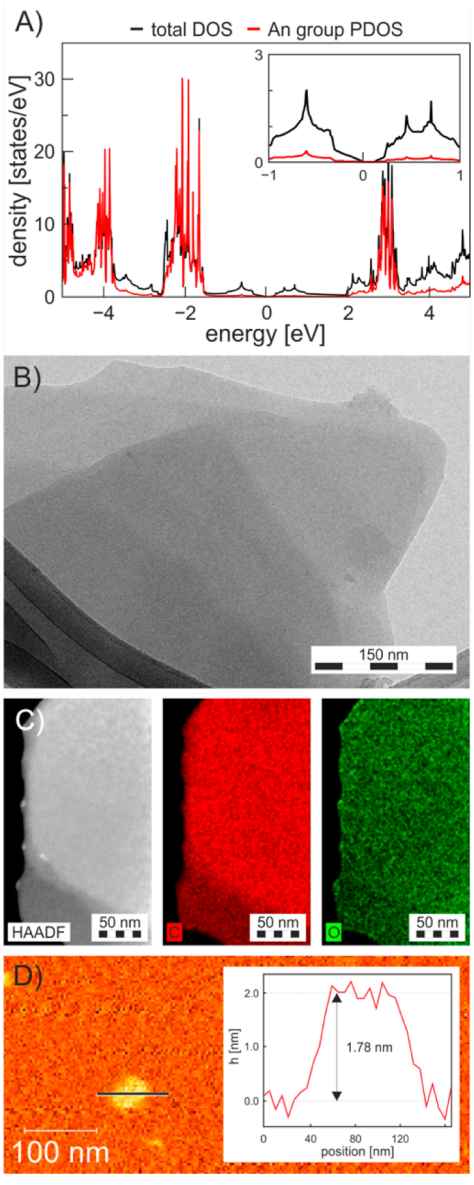

Figure 3. (A) Density of states of AnG. (B) TEM and (C) dark field image with carbon and oxygen EDS maps of AnG flakes. (D) AFM image with the height profile of a typical AnG flake.

sp^3 defects in the graphene lattice because the molecular states lay 3 eV (AlG and AnG) and 5 eV (PeG) below the Fermi level (Figure 3A). The optical BGs were also evaluated experimentally from the Tauc plots (Figure S5). Both experimental and theoretical BG values displayed the same trend: BG_{PeG} > BG_{AlG} > BG_{AnG}, although BG depended on the functional group rather weakly. The lengths of the C−C bonds between the sp^3 lattice-carbons and the carbons of the functional groups were 1.62 Å, 1.61 and 1.59 Å for pentyl, allyl and anisolyl, respectively, and correlated with the binding energies. The lengths of the new C−C bonds were somewhat longer than a typical single $C(sp^3)$−$C(sp^3)$ bond of 1.54 Å, indicating that their bond orders were slightly below one, and thus they were susceptible to detachment from the graphene surface.

In TGA, the PeG, AlG and AnG derivatives lost 45%, 42.5% and 44% of their weight, respectively, between 200 and 580 °C. The weight losses corresponded to detachment of the functional groups, as suggested by the DFT calculations. This was also confirmed for the PeG derivative by mass spectroscopy analysis of the evolved gases and, in particular, by the detection of a fragment at m/z 71 corresponding to the pentyl group ($M_r(C_5H_{11})$ = 71.1, Figure S3). Considering that the weight losses corresponded to detachment of the functional groups, we assessed the degree of functionalization (DF, see S.I. for details) of the individual graphene derivatives to be 8.5, 11.2, and 5.5%, for PeG, AlG and AnG, respectively. The presence of impurities detected by XPS was also taken into account when determining the DF. Such DF values are particularly high when compared to graphene derivatives synthesized by reactions on graphene. For example, values of 1.2 to 5% DF were obtained after reaction with diazonium salts.[31,35,36] Importantly, the high DF of FG resulted in high dispersibility of the adducts in organic solvents (Figure S6).

Finally, we examined the morphology of the graphene derivatives by transmission electron microscopy (TEM), atomic force microscopy (AFM) and energy dispersive spectroscopy (EDS) elemental mapping. All prepared materials exhibited similar morphological characteristics (Figures 3 and S7). A representative TEM image of AnG (Figure 3B) showed that the functionalized material consisted of flakes containing very few layers. AFM measurements indicated that the thickness of AnG was around 1.8 nm (Figure 3D), which corresponded well to the thickness of double-side-functionalized graphene by the anisol group estimated by DFT calculations (1.77 nm). AFM analysis on AlG verified the few-layer nature of the flakes (Figure S8). EDS elemental mapping verified the presence of oxygen on the graphene lattice with a homogeneous distribution of oxygen over the graphene surface (Figure 3C).

In conclusion, a straightforward, facile and very efficient approach for the covalent double-sided and high-degree functionalization of graphene was developed. This was achieved by exfoliation of the commercially available material graphite fluoride and its reaction with Grignard reagents. In three cases, nucleophilic substitution on FG was successful and alkylated, alkenylated and arylated graphene derivatives were prepared under mild reaction conditions. Concurrent reductive defluorination allowed the preparation of fluorine-free and well-defined graphene derivatives, which were highly dispersible in organic solvents. The reaction resulted in the homogeneous, high-degree (5.5−11.2%) and double-sided functionalization of graphene. Moreover, we verified through theoretical calculations that the value of nucleophilicity governs the success of nucleophilic substitution on FG. The prepared allyl derivative is

DOI: 10.1021/acs.chemmater.6b05040
Chem. Mater. 2017, 29, 926−930

particularly interesting because the presence of the double bond enables further chemical reactions.[37−39] Therefore, a wide range of successive graphene derivatives could be prepared starting from the allyl graphene.

■ ASSOCIATED CONTENT

Supporting Information

The Supporting Information is available free of charge on the ACS Publications website at DOI: 10.1021/acs.chemmater.6b05040.

Experimental and calculation details, and supporting figures (PDF)

■ AUTHOR INFORMATION

Corresponding Author

*E-mail: Michal.Otyepka@upol.cz; Tel: +420 585 634 756.

ORCID

Radek Zbořil: 0000-0002-3147-2196

Michal Otyepka: 0000-0002-1066-5677

Notes

The authors declare no competing financial interest.

■ ACKNOWLEDGMENTS

We thank O. Tomanec for HR-TEM and EDS, M. Petr for XPS, S. Štěpánková for Raman, J. P. Froning for AFM and J. Ugolotti for TGA. We acknowledge financial support from the Ministry of Education, Youth and Sports of the Czech Republic (Grants LO1305, CZ.1.05/2.1.00/19.0377 and the Research Infrastructure NanoEnviCz: project No. LM2015073), the ERC (Consolidator grant 683024 from the European Union's Horizon 2020 research and innovation programme), and the Neuron fund.

■ REFERENCES

(1) Georgakilas, V.; Otyepka, M.; Bourlinos, A. B.; Chandra, V.; Kim, N.; Kemp, K. C.; Hobza, P.; Zbořil, R.; Kim, K. S. Functionalization of Graphene: Covalent and Non-Covalent Approaches, Derivatives and Applications. *Chem. Rev.* **2012**, *112*, 6156−6214.

(2) Criado, A.; Melchionna, M.; Marchesan, S.; Prato, M. The Covalent Functionalization of Graphene on Substrates. *Angew. Chem., Int. Ed.* **2015**, *54*, 10734−10750.

(3) Eigler, S.; Hirsch, A. Chemistry with Graphene and Graphene Oxide—Challenges for Synthetic Chemists. *Angew. Chem., Int. Ed.* **2014**, *53*, 7720−7738.

(4) Jeon, I.-Y.; Bae, S.-Y.; Seo, J.-M.; Baek, J.-B. Scalable Production of Edge-Functionalized Graphene Nanoplatelets via Mechanochemical Ball-Milling. *Adv. Funct. Mater.* **2015**, *25*, 6961−6975.

(5) Baraket, M.; Walton, S. G.; Lock, E. H.; Robinson, J. T.; Perkins, F. K. The Functionalization of Graphene Using Electron-Beam Generated Plasmas. *Appl. Phys. Lett.* **2010**, *96*, 231501.

(6) Lee, W. H.; Suk, J. W.; Lee, J.; Hao, Y.; Park, J.; Yang, J. W.; Ha, H.-W.; Murali, S.; Chou, H.; Akinwande, D.; Kim, K. S.; Ruoff, R. S. Simultaneous Transfer and Doping of CVD-Grown Graphene by Fluoropolymer for Transparent Conductive Films on Plastic. *ACS Nano* **2012**, *6*, 1284−1290.

(7) Lee, W. H.; Suk, J. W.; Chou, H.; Lee, J.; Hao, Y.; Wu, Y.; Piner, R.; Akinwande, D.; Kim, K. S.; Ruoff, R. S. Selective-Area Fluorination of Graphene with Fluoropolymer and Laser Irradiation. *Nano Lett.* **2012**, *12*, 2374−2378.

(8) Wang, Q. H.; Jin, Z.; Kim, K. K.; Hilmer, A. J.; Paulus, G. L. C.; Shih, C.-J.; Ham, M.-H.; Sanchez-Yamagishi, J. D.; Watanabe, K.; Taniguchi, T.; Kong, J.; Jarillo-Herrero, P.; Strano, M. S. Understanding and Controlling the Substrate Effect on Graphene Electron-Transfer Chemistry via Reactivity Imprint Lithography. *Nat. Chem.* **2012**, *4*, 724−732.

(9) Fan, X.; Nouchi, R.; Tanigaki, K. Effect of Charge Puddles and Ripples on the Chemical Reactivity of Single Layer Graphene Supported by SiO2/Si Substrate. *J. Phys. Chem. C* **2011**, *115*, 12960−12964.

(10) Sharma, R.; Baik, J. H.; Perera, C. J.; Strano, M. S. Anomalously Large Reactivity of Single Graphene Layers and Edges toward Electron Transfer Chemistries. *Nano Lett.* **2010**, *10*, 398−405.

(11) Koehler, F. M.; Jacobsen, A.; Ensslin, K.; Stampfer, C.; Stark, W. J. Selective Chemical Modification of Graphene Surfaces: Distinction Between Single- and Bilayer Graphene. *Small* **2010**, *6*, 1125−1130.

(12) Diankov, G.; Neumann, M.; Goldhaber-Gordon, D. Extreme Monolayer-Selectivity of Hydrogen-Plasma Reactions with Graphene. *ACS Nano* **2013**, *7*, 1324−1332.

(13) Nair, R. R.; Ren, W.; Jalil, R.; Riaz, I.; Kravets, V. G.; Britnell, L.; Blake, P.; Schedin, F.; Mayorov, A. S.; Yuan, S.; Katsnelson, M. I.; Cheng, H.-M.; Strupinski, W.; Bulusheva, L. G.; Okotrub, A. V.; Grigorieva, I. V.; Grigorenko, A. N.; Novoselov, K. S.; Geim, A. K. Fluorographene: A Two-Dimensional Counterpart of Teflon. *Small* **2010**, *6*, 2877−2884.

(14) Zbořil, R.; Karlický, F.; Bourlinos, A. B.; Steriotis, T. A.; Stubos, A. K.; Georgakilas, V.; Šafářová, K.; Jančík, D.; Trapalis, C.; Otyepka, M. Graphene Fluoride: A Stable Stoichiometric Graphene Derivative and Its Chemical Conversion to Graphene. *Small* **2010**, *6*, 2885−2891.

(15) Robinson, J. T.; Burgess, J. S.; Junkermeier, C. E.; Badescu, S. C.; Reinecke, T. L.; Perkins, F. K.; Zalalutdniov, M. K.; Baldwin, J. W.; Culbertson, J. C.; Sheehan, P. E.; Snow, E. S. Properties of Fluorinated Graphene Films. *Nano Lett.* **2010**, *10*, 3001−3005.

(16) Nair, R. R.; Sepioni, M.; Tsai, I.-L.; Lehtinen, O.; Keinonen, J.; Krasheninnikov, A. V.; Thomson, T.; Geim, A. K.; Grigorieva, I. V. Spin-Half Paramagnetism in Graphene Induced by Point Defects. *Nat. Phys.* **2012**, *8*, 199−202.

(17) Karlický, F.; Kumara, R. D.; Otyepka, M.; Zbořil, R. Halogenated Graphenes: Rapidly Growing Family of Graphene Derivatives. *ACS Nano* **2013**, *7*, 6434−6464.

(18) Feng, W.; Long, P.; Feng, Y.; Li, Y. Two-Dimensional Fluorinated Graphene: Synthesis, Structures, Properties and Applications. *Adv. Sci.* **2016**, *3*, No. 1500413.

(19) Dubecký, M.; Otyepková, E.; Lazar, P.; Karlický, F.; Petr, M.; Čépe, K.; Banáš, P.; Zbořil, R.; Otyepka, M. Reactivity of Fluorographene: A Facile Way toward Graphene Derivatives. *J. Phys. Chem. Lett.* **2015**, *6*, 1430−1434.

(20) Urbanová, V.; Holá, K.; Bourlinos, A. B.; Čépe, K.; Ambrosi, A.; Loo, A. H.; Pumera, M.; Karlický, F.; Otyepka, M.; Zbořil, R. Thiofluorographene-Hydrophilic Graphene Derivative with Semiconducting and Genosensing Properties. *Adv. Mater.* **2015**, *27*, 2305−2310.

(21) Stine, R.; Ciszek, J. W.; Barlow, D. E.; Lee, W.-K.; Robinson, J. T.; Sheehan, P. E. High-Density Amine-Terminated Monolayers Formed on Fluorinated CVD-Grown Graphene. *Langmuir* **2012**, *28*, 7957−7961.

(22) Whitener, K. E., Jr.; Stine, R.; Robinson, J. T.; Sheehan, P. E. Graphene as Electrophile: Reactions of Graphene Fluoride. *J. Phys. Chem. C* **2015**, *119*, 10507−10512.

(23) Bosch-Navarro, C.; Walker, M.; Wilson, N. R.; Rourke, J. P. Covalent Modification of Exfoliated Fluorographite with Nitrogen Functionalities. *J. Mater. Chem. C* **2015**, *3*, 7627−7631.

(24) Li, B.; He, T.; Wang, Z.; Cheng, Z.; Liu, Y.; Chen, T.; Lai, W.; Wang, X.; Liu, X. Chemical Reactivity of C-F Bonds Attached to Graphene with Diamines Depending on Their Nature and Location. *Phys. Chem. Chem. Phys.* **2016**, *18*, 17495−17505.

(25) Lazar, P.; Chua, C. K.; Holá, K.; Zbořil, R.; Otyepka, M.; Pumera, M. Dichlorocarbene-Functionalized Fluorographene: Synthesis and Reaction Mechanism. *Small* **2015**, *11*, 3790−3796.

(26) Ye, X.; Ma, L.; Yang, Z.; Wang, J.; Wang, H.; Yang, S. Covalent Functionalization of Fluorinated Graphene and Subsequent Application as Water-Based Lubricant Additive. *ACS Appl. Mater. Interfaces* **2016**, *8*, 7483−7488.

DOI: 10.1021/acs.chemmater.6b05040
Chem. Mater. 2017, 29, 926−930

(27) Boul, P. J.; Liu, J.; Mickelson, E. T.; Huffman, C. B.; Ericson, L. M.; Chiang, I. W.; Smith, K. A.; Colbert, D. T.; Hauge, R. H.; Margrave, J. L.; Smalley, R. E. Reversible Sidewall Functionalization of Buckytubes. *Chem. Phys. Lett.* **1999**, *310*, 367−372.
(28) Hossain, M. Z.; Razak, M. B. A.; Noritake, H.; Shiozawa, Y.; Yoshimoto, S.; Mukai, K.; Koitaya, T.; Yoshinobu, J.; Hosaka, S. Monolayer Selective Methylation of Epitaxial Graphene on SiC(0001) through Two-Step Chlorination−Alkylation Reactions. *J. Phys. Chem. C* **2014**, *118*, 22096−22101.
(29) Hossain, M. Z.; Razak, M. B. A. Halogenation of Epitaxial Graphene Grown on the Si-Face of the SiC(0001) Substrate and Its Further Reaction with Grignard Reagent. *New J. Chem.* **2016**, *40*, 1671−1678.
(30) Bourlinos, A. B.; Šafářová, K.; Šišková, K.; Zbořil, R. The Production of Chemically Converted Graphenes from Graphite Fluoride. *Carbon* **2012**, *50*, 1425−1428.
(31) Englert, J. M.; Dotzer, C.; Yang, G.; Schmid, M.; Papp, C.; Gottfried, J. M.; Steinrück, H.-P.; Spiecker, E.; Hauke, F.; Hirsch, A. Covalent Bulk Functionalization of Graphene. *Nat. Chem.* **2011**, *3*, 279−286.
(32) Englert, J. M.; Vecera, P.; Knirsch, K. C.; Schäfer, R. A.; Hauke, F.; Hirsch, A. Scanning-Raman-Microscopy for the Statistical Analysis of Covalently Functionalized Graphene. *ACS Nano* **2013**, *7*, 5472−5482.
(33) Karlický, F.; Zbořil, R.; Otyepka, M. Band Gaps and Structural Properties of Graphene Halides and Their Derivates: A Hybrid Functional Study with Localized Orbital Basis Sets. *J. Chem. Phys.* **2012**, *137*, 034709.
(34) Karlický, F.; Otyepka, M. Band Gaps and Optical Spectra of Chlorographene, Fluorographene and Graphane from G0W0, GW0 and GW Calculations on Top of PBE and HSE06 Orbitals. *J. Chem. Theory Comput.* **2013**, *9*, 4155−4164.
(35) Lomeda, J. R.; Doyle, C. D.; Kosynkin, D. V.; Hwang, W.-F.; Tour, J. M. Diazonium Functionalization of Surfactant-Wrapped Chemically Converted Graphene Sheets. *J. Am. Chem. Soc.* **2008**, *130*, 16201−16206.
(36) Zhu, Y.; Higginbotham, A. L.; Tour, J. M. Covalent Functionalization of Surfactant-Wrapped Graphene Nanoribbons. *Chem. Mater.* **2009**, *21*, 5284−5291.
(37) Wei, J.; Qiu, J. Allyl-Functionalization Enhanced Thermally Stable Graphene/Fluoroelastomer Nanocomposites. *Polymer* **2014**, *55*, 3818−3824.
(38) Rodier, B. J.; Mosher, E. P.; Burton, S. T.; Matthews, R.; Pentzer, E. Polythioether Particles Armored with Modifiable Graphene Oxide Nanosheets. *Macromol. Rapid Commun.* **2016**, *37*, 894−899.
(39) Roy, S.; Das, T.; Zhang, L.; Hu, X. M. Harnessing the Maximum Reinforcement of Graphene Oxide for Poly(vinylidene Fluoride) Nanocomposites via Polydopamine Assisted Novel Surface Modification. *RSC Adv.* **2016**, *6*, 69919−69929.

DOI: 10.1021/acs.chemmater.6b05040
Chem. Mater. 2017, 29, 926−930